J Therm Anal Calorim (2013) 112:1325–1333
DOI 10.1007/s10973-012-2688-5

Preparation, characterization and thermal dehydration kinetics of titanate nanotubes

Müge Sarı Yılmaz · Sibel Kasap · Sabriye Pişkin

Received: 17 April 2012 / Accepted: 4 September 2012 / Published online: 9 October 2012

Abstract Titanate nanotubes were synthesized utilizing the hydrothermal method using titanium dioxide nanoparticles. The experiments were carried out considering the process as a function of reaction temperature, time, NaOH concentration and the acidity of the washing solution. The formation of titanate nanotubes was shown to be affected strongly by variations in any parameter. The optimum conditions for the synthesis of titanate nanotubes were determined to be a reaction temperature of 190 °C, and a reaction time of 12 h, using 10 M NaOH concentration and the washing solution to have a pH of 5.5. In addition, thermogravimetric analysis (TG/DTG) was used to investigate the thermal behaviour and dehydration kinetics of titanate nanotubes. In order to better understand their thermal behaviour, the thermal analysis of bulk hydrogen trititanate was performed. The values of the apparent activation energies of the first and second dehydration stages for titanate nanotubes were 81.44 ± 15.85 and 82.69 ± 7.46 kJ mol^{-1}, respectively. The values of the apparent activation energies of the first, second and third dehydration stages for bulk hydrogen trititanate were 115.93 ± 5.40, 137.58 ± 6.47 and 138.97 ± 8.47 kJ mol^{-1}, respectively.

Keywords Titanate nanotubes · Bulk hydrogen trititanate · Dehydration kinetics · Model-free method

M. Sarı Yılmaz · S. Pişkin (✉)
Faculty of Chemical and Metallurgical Engineering, Yıldız Technical University, Davutpasa Campus, Istanbul, Turkey
e-mail: piskin@yildiz.edu.tr

S. Kasap
Faculty of Engineering and Natural Sciences, Sabancı University, Istanbul, Turkey

Introduction

Nano-sized materials have received increasing attention in various fields owing to the virtue of their special chemical and physical properties. Much work has recently been done on the synthesis and the applications of nano-sized metal oxides such as TiO_2, ZnO, SiO_2 and similar compounds due to their peculiar catalytic behaviours, nonlinear optical properties and unusual luminescence responses [1]. Amongst these materials, nano-sized TiO_2 has attracted a lot of interest from the industry as well as from the scientific community. This is a result of the very nature of titanium dioxide nanomaterials, which have many interesting properties, such as high oxidative power, nontoxicity, photo-stability, water insolubility, wide band gap, high refractive index and the ability to function as a photo catalyst under UV radiation. These properties have resulted in the wide use of titania in many industries and various other applications [2].

Moreover, the discovery of carbon nanotubes [3] intrigued the intensive researches regarding one-dimensional nanostructures, such as nanotubes, nanorods, nanowires and nanobelts. TiO_2-based nanotubes, therefore, attracted extensive and engrossing interest despite their crystalline structure still being controversial. The present controversy about it is amongst the following: Tetragonal anatase TiO_2 [4], monoclinic $H_2Ti_3O_7$ [3], orthorhombic $H_2Ti_2O_5{\cdot}H_2O$ [5], lepidocrocite $H_xTi_{2-x/4}\square_{x/4}O_4$ ($x \sim 0.7$, $\square$: vacancy) [6] and monoclinic $H_2Ti_4O_9.H_2O$ [7] have been proposed to represent the crystal structure of the nanotubes. According to the literature, the chemical compositions of $Na_xH_{2-x}Ti_3O_7$ and $Na_xH_{2-x}Ti_2O_4(OH)$ groups are more acceptable than other structures [8].

TiO_2-based nanotubes with their high specific surface area, ion- exchangeability and photo catalytic ability were

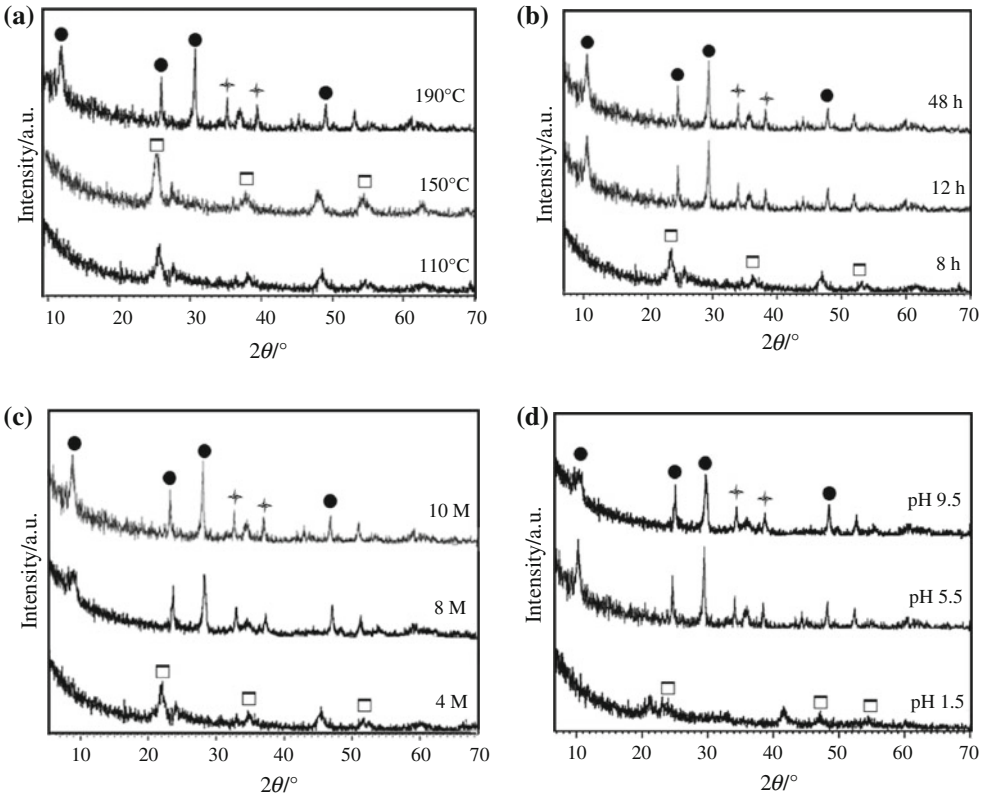

Fig. 1 XRD patterns of TNTs prepared at various **a** temperatures, **b** reaction times, **c** concentration of NaOH solution and **d** pH of washing solutions (*filled circle* titanate nanotubes, *open square* anatase, and + rutile)

considered for use in extensive applications such as support/carriers, ion-exchange/adsorption, photochemistry and dry sensitized solar cells [8]. Currently, developed methods of fabricating TiO_2-based nanotubes comprise of the assisted-template method [9, 10], the sol–gel process [11], electrochemical anodic oxidation [12, 13] and hydrothermal treatment [4, 14]. Amongst them, the hydrothermal technique is widely employed to prepare titanate nanotubes by treating the TiO_2 powder precursors in alkali aqueous solution [15]. However, this process usually requires 20–72 h at the temperature of 110–160 °C [3, 16, 17].

In recent years, thermogravimetry has been commonly used for studying the kinetic parameters of nano-sized materials [18–22]. To our knowledge, limited research has been published on the thermal kinetics of titanate nanotubes (TNTs). Xie et al. [23] reported that the activation energy for dehydration of hydrogen titanate nanotube prepared by potassium dititanate with water vapour treatment is 60 kJ mol^{-1} in the range of $0.1 < \alpha < 0.7$ according to the Friedman and Flynn–Wall–Ozawa models.

This study also focused on the synthesis of TNTs with smaller diameters directly from TiO_2 powders using a hydrothermal technique with a shorter reaction time than in previous studies. The effects of the reaction temperature, the reaction time, NaOH concentration and the acidity of the washing solution on the crystalline transformation were determined. After obtaining the optimum parameters, TNTs were synthesized and then characterized by different analysis techniques. The kinetic analysis of TNTs was performed using the Vyazovkin model-free method. In addition, the thermal analysis of bulk hydrogen trititanate (BHT) was performed in order to better understand the thermal behaviour of TNTs.

Experimental

Preparation of TNTs

Anatase TiO_2 powder having an average particle diameter of 17 nm [24] was used as the starting material for the preparation of TNTs via the hydrothermal method. 0.5 g of powder was added to 40 mL of NaOH solutions of varying molarity between 4 and 10 M in a Teflon vessel with rigorous stirring and the obtained mixture was placed into a Teflon-lined autoclave vessel of 125 mL volume. Finally, the autoclave was sealed and placed in the oven, operating at a temperature varying in the range of 110–190 °C, and thus also changing the reaction time for the synthesis of TNTs. The resulting slurry was initially rinsed with deionized water. Then, the precipitate was washed thoroughly with either aqueous HCl or aqueous NaOH solution

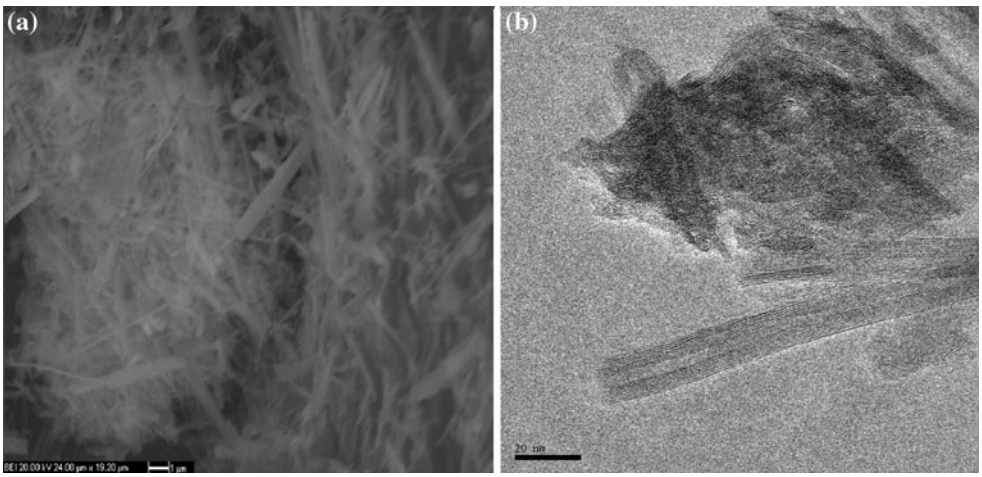

Fig. 2 **a** SEM image and **b** HRTEM image for TNTs with 10 M NaOH concentration at 190 °C for 12 h

at different pH values and finally, TNTs were washed with deionized water so that the pH value was maintained at 7.

Preparation of BHT

After preparing the TNTs at optimum conditions, bulk titanate samples were synthesized by the solid state reaction and their thermal behaviour was investigated and compared to that of TNTs. The bulk hydrogen trititanate samples were synthesized according to the method from a previous study [25], with some modifications. Firstly, $Na_2Ti_3O_7$ powders were prepared by a solid state reaction of Na_2CO_3 and anatase TiO_2. A mixture in a molar ratio of Na_2CO_3:TiO_2 = 1:3 was heated at 800 °C for 25 h in a platinum crucible. At the end of the time, the obtained $Na_2Ti_3O_7$ powder (ca. 1 g) was cooled to room temperature and then transferred to 100 mL 0.1 M HCl. The mixture was placed in a shaking water bath at 25 °C for 4 days with the acid solution changed daily to completely remove alkalinity from the reaction product. Finally, the powder was washed with deionized water and dried at 110 °C.

Characterization

The crystalline structures of TNTs and BHT were analysed using a Philips Panalytical X'Pert-Pro diffractometer (CuKα radiation with $\lambda = 1.5418$ Å at 45 kV/40 mA). A scanning electron microscope (SEM; CamScan Apollo 300) was used to observe the morphology as well as the crystallinity of TNTs. High Resolution Transmission Electron Microscopy (HRTEM; JEOL 2100 LaB6) was utilized to view the internal structure/morphology of the formed nanotubes. The thermal analyses of TNTs and BHT were carried out using a Perkin Elmer Pyris Diamond thermal analysis equipment under a constant nitrogen flow of 200 mL min^{-1} at different heating rates (5, 15 and 20 °C min^{-1}).

Theoretical background

In this study, the Vyazovkin model-free kinetic method was employed in order to investigate the kinetic parameters for the dehydration processes of TNTs and BHT. With this method, accurate evaluations of complex reactions are performed as a way of obtaining reliable consistent kinetic information about the overall process [26]. Vyazovkin developed an advanced isoconversional method, wherein no model has to be selected, that allows evaluation of thermal degradation reactions using different heating rates. The theory is based on the idea that the activation energy is constant for a certain conversion (isoconversional method). A chemical reaction is measured at least three different heating rates (β) and the respective conversion curves are determined [27, 28]. This method is based on the equation

$$\frac{d\alpha}{dt} = k.f(\alpha) \tag{1}$$

where $f(\alpha)$ represents the reaction model, k is the velocity constant (s^{-1}) and α is the conversion degree. Taking the reaction rate equation, presented as $f(\alpha)$ and dividing by the heating rate $\beta = dT/dt$, one obtains

$$\frac{d\alpha}{dt} = kf(\alpha) \Rightarrow \frac{d\alpha}{dT} = \frac{k}{\beta}f(\alpha) \tag{2}$$

Replacing k on Eq. (2) with the Arrhenius expression ($k = k_0 e^{-E/RT}$) and rearranging it gives

$$\frac{1}{f(\alpha)}d\alpha = \frac{k_0}{\beta}e^{-E/RT}dT \tag{3}$$

Integrating Eq. (3) gives

$$\int_0^{\alpha}\frac{1}{f(\alpha)}d\alpha = g(\alpha) = \frac{k_0}{\beta}\int_{T_0}^{T} e^{-\frac{E}{RT}}dT \tag{4}$$

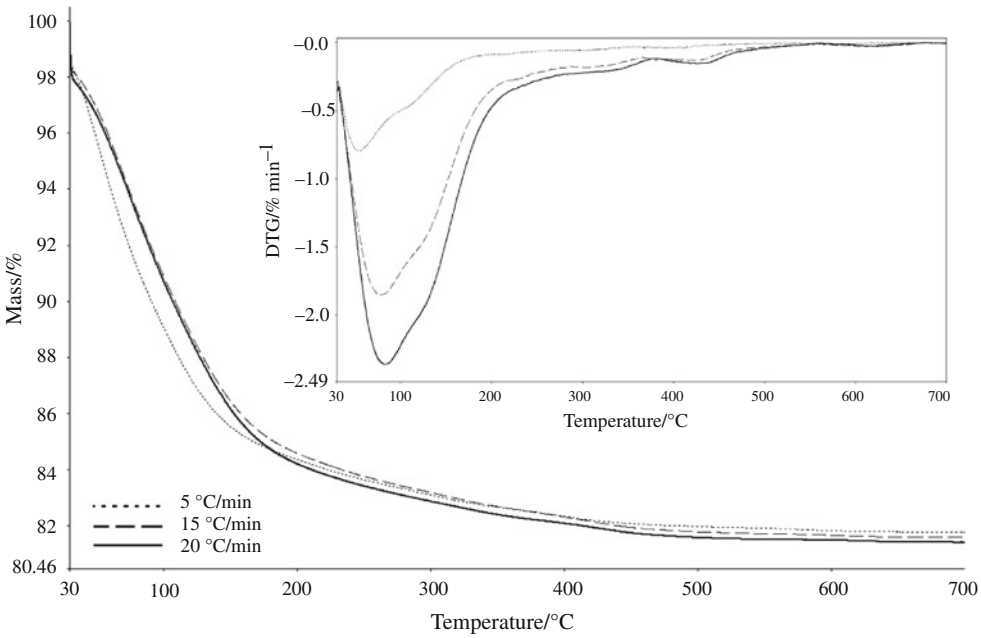

Fig. 3 TG/DTG curve for TNTs at different heating rates

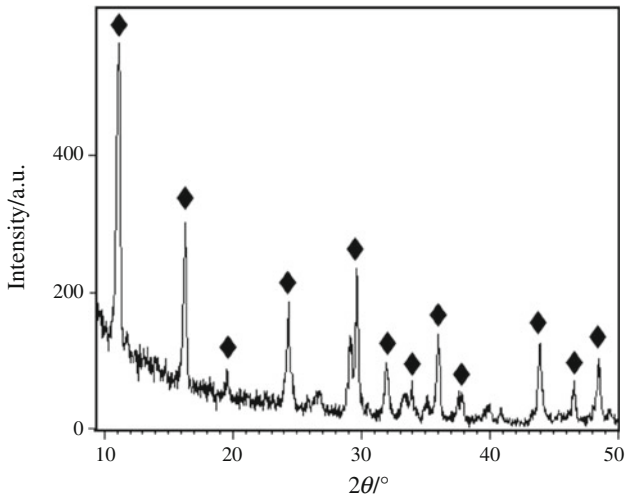

Fig. 4 XRD pattern of BHT

Since $E/RT \gg 1$, the temperature integral can be approximated by

$$\int_{T_0}^{T} e^{-E/RT} dT \approx \frac{R}{E} T^2 e^{-E/RT} \quad (5)$$

Finally, substituting Eq. (5) on Eq. (4), rearranging and logarithming, we obtain

$$\ln \frac{\beta}{T_\alpha^2} = \ln \left[\frac{Rk_0}{E_a g(\alpha)} \right] - \frac{E_a}{R} \frac{1}{T_\alpha} \quad (6)$$

Eq. (6) is a dynamic equation that was applied for the determination of the activation energy (E_a) for all conversion degrees (α).

Results and discussions

Studies of preparation conditions

Effect of reaction temperature

Figure 1a shows the results of the XRD analysis of the products formed using anatase TiO_2 as the starting material being hydrothermally treated in a 10 M NaOH solution at various reaction temperatures for 48 h. As it is shown in the figure, the peak at $2\theta = 25.5$ from (101) of anatase TiO_2 was observed to occur at 110–150 °C. However, the pattern of the particles obtained from the samples treated at the 190 °C reaction temperature indicated that the ($2\theta \approx 10$) characteristic peak [16] corresponding to TNTs appeared. It means that if the reaction was conducted at that temperature, titanium dioxide nanoparticles would be transformed into TNTs.

Effect of reaction time

The XRD patterns of the TNTs synthesized at 190 °C with varying reaction time and using 10 M NaOH solution are shown in Fig. 1b. All XRD peaks belonging to titanate nanoparticles were assigned to the anatase phase at the 8th hour, whereas the peaks belonging to the particles obtained at the 12th hour showed different results. The characteristic peaks of anatase titanium dioxide disappeared and were replaced by new peaks corresponding to TNTs. It could be concluded that the reaction time for the transformation of titanium dioxide nanoparticles to TNTs was found to be 12 h. The reaction time previously reported for this reaction

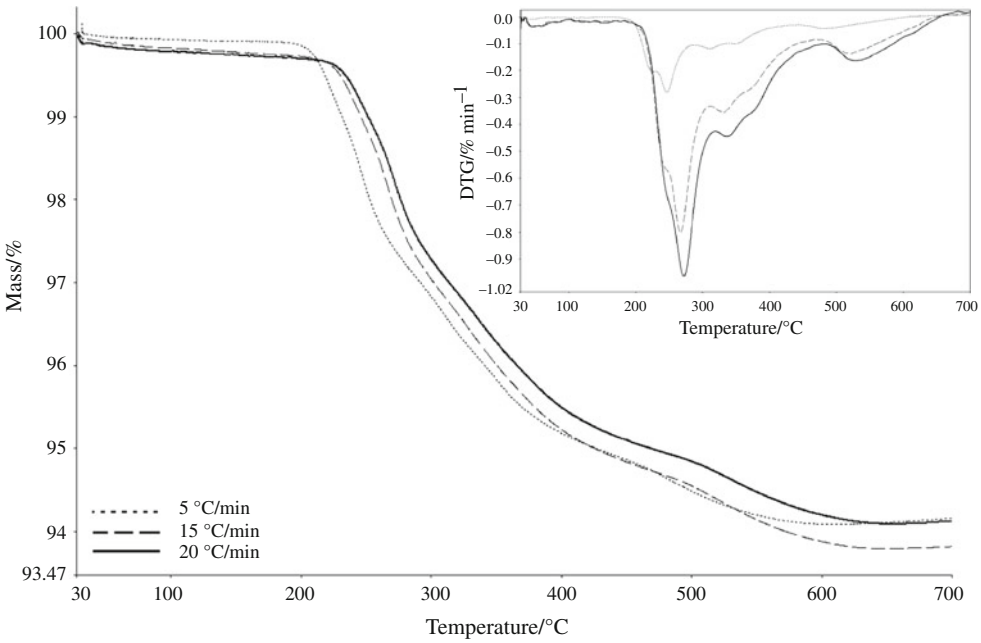

Fig. 5 TG/DTG curve for BHT at different heating rates

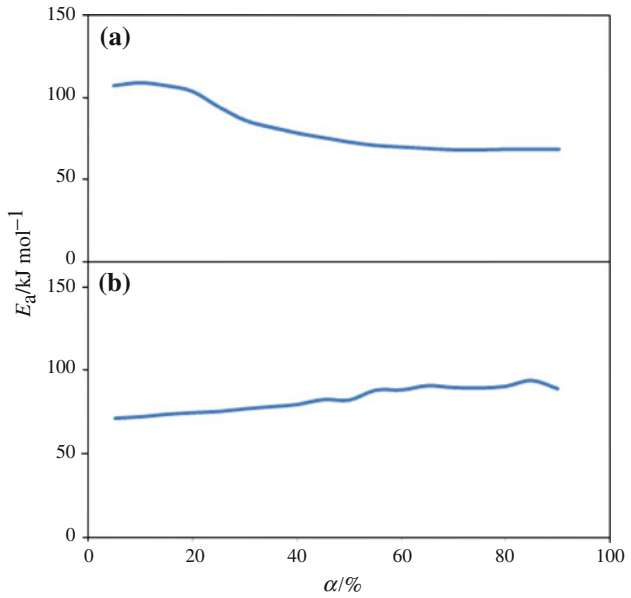

Fig. 6 Activation energy as a function of conversion for dehydration processes of TNTs **a** first stage, **b** second stage

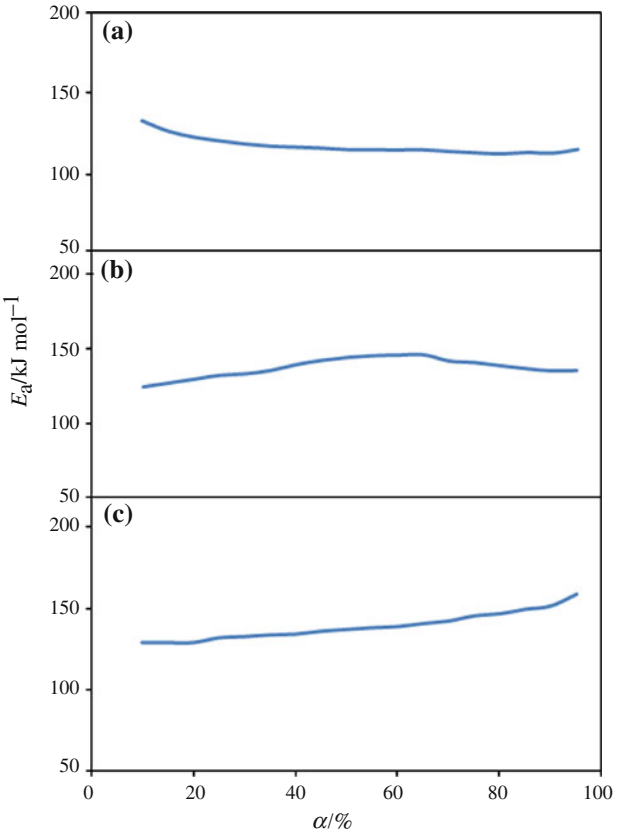

Fig. 7 Activation energy as a function of conversion for dehydration processes of BHT **a** first stage, **b** second stage and **c** third stage

which was carried out at 110–180 °C was observed to change between 20 and 72 h [3, 17, 18]. This variation in the reaction time may be attributed to the crystallite size of TiO_2 synthesized by a sonochemical reaction.

Effect of NaOH concentration

Figure 1c shows the results of the XRD analysis for TNTs synthesized at 190 °C for 12 h using various concentrations of NaOH solutions. The treatment at 190 °C led to the formation of needle-shaped products when NaOH aqueous solution with the concentration of 8 or 10 M was used.

Table 1 Temperature for dehydration of TNTs as a function of the time for different conversions

Time/min	Conversion/%						
	10	25	50	75	90	95	99
First step							
10	42.91	55.05	70.78	86.61	97.20	100.90	104.06
30	42.75	54.76	70.16	85.61	95.95	99.58	102.68
60	42.66	54.58	69.77	84.99	95.18	98.77	101.83
90	42.60	54.47	69.55	84.63	94.74	98.30	101.33
120	42.56	54.40	69.39	84.38	94.42	97.98	100.99
150	42.53	54.34	69.26	84.19	94.18	97.72	100.72
180	42.50	54.29	69.16	84.03	93.98	97.51	100.50
210	42.48	54.25	69.08	83.90	93.82	97.34	100.32
240	42.46	54.21	69.00	83.78	93.67	97.18	100.16
270	42.45	54.18	68.94	83.68	93.55	97.06	100.02
300	42.43	54.15	68.89	83.59	93.44	96.94	99.90
360	42.41	54.11	68.79	83.43	93.24	96.73	99.68
Second step							
10	112.47	125.07	153.71	240.29	354.60	405.80	530.98
30	110.90	123.20	151.13	234.54	342.17	392.74	503.90
60	109.92	122.05	149.55	231.05	334.76	384.93	488.19
90	109.36	121.39	148.65	229.06	330.58	380.50	479.45
120	108.97	120.93	148.01	227.67	327.67	377.42	473.43
150	108.67	120.57	147.52	226.60	325.45	375.07	468.87
180	108.42	120.28	147.12	225.73	323.66	373.17	465.21
210	108.21	120.03	146.78	225.00	322.16	371.57	462.16
240	108.03	119.82	146.49	224.38	320.87	370.20	459.54
270	107.87	119.64	146.24	223.83	319.75	369.00	457.26
300	107.73	119.47	146.01	223.34	318.75	367.94	455.24
360	107.49	119.18	145.62	222.50	317.03	366.11	451.79

However, when a solution with the concentration of 4 M was used, the products were not formed by the treatment for 12 h. Dilute NaOH aqueous solution has a poor ability to form the tubular-shaped products. Additionally, as the concentration of the NaOH solution increased, the peak intensities for the TNTs increased, indicating better performance of crystallinity for the nanotube structure.

Effect of the acidity of the washing solution treatment

Figure 1d shows the results of the XRD analysis of the sample synthesized at 190 °C for 12 h in 10 M NaOH solution following the addition of either HCl or NaOH solution. If the pH was 5.5 or 9.5, a characteristic peak would be observed at approximately $2\theta \approx 10$, which would be considered to correspond to the titanate nanotube crystals. On the other hand, if the pH was 1.5, a peak observed at approximately $2\theta \approx 10$ would not exist.

By controlling the acidity of the washing solution treatment, it was possible to form either titania or TNTs. In addition, it would be expected that a new type of titania nanotube having novel properties would be formed by controlling the amount of residual Na^+ ions and by replacing the residual Na^+ ions with other ions [16].

Characterization of TNTs

Figure 2a shows the SEM evaluation of the product synthesized under optimum reaction conditions. High purity nanotubes were entangled together. Figure 2b depicts a HRTEM image demonstrating uniform nanotubes with inner diameters of ca. 4 nm and outer diameters of ca. 12 nm. Also, the investigation of the HRTEM images revealed that the nanotubes were usually five layers thick.

The TG/DTG curves of the TNTs showed mass losses in two dehydration stages in the range of 30–630 °C at 15 °C min^{-1} heating (Fig. 3). The first mass loss occurred between 30 and 110 °C with a mass loss of 8.55 % which was usually attributed to the adsorbed water and interlayer water, followed by the final dehydration with a mass loss of 8.17 % corresponded to dehydroxylation of the nanotubes.

Table 2 Temperature for dehydration of BHT as a function of the time for different conversions

Time/min	Conversion/%						
	10	25	50	75	90	95	99
First step							
10	216.94	229.51	246.87	261.24	275.65	282.17	287.56
30	213.72	225.54	242.07	255.77	269.56	275.92	281.15
60	211.74	223.11	239.13	252.44	265.85	272.12	277.26
90	210.60	221.71	237.45	250.53	263.73	269.94	275.02
120	209.79	220.73	236.27	249.19	262.25	268.42	273.46
150	209.17	219.97	235.36	248.16	261.11	267.25	272.26
180	208.67	219.36	234.63	247.33	260.18	266.30	271.29
210	208.25	218.84	234.01	246.63	259.41	265.51	270.48
240	207.88	218.40	233.47	246.03	258.74	264.82	269.77
270	207.56	218.01	233.00	245.50	258.15	264.22	269.16
300	207.27	217.66	232.59	245.03	257.63	263.68	268.61
360	206.78	217.06	231.87	244.21	256.73	262.76	267.66
Second step							
10	299.32	313.66	339.80	370.66	401.48	416.05	429.29
30	292.89	307.02	332.65	361.97	390.89	404.71	417.05
60	288.97	302.97	328.29	356.69	384.49	397.86	409.67
90	286.73	300.65	325.79	353.67	380.85	393.97	405.48
120	285.16	299.02	324.04	351.56	378.30	391.25	402.56
150	283.95	297.77	322.70	349.94	376.35	389.16	400.32
180	282.98	296.76	321.61	348.63	374.77	387.48	398.51
210	282.15	295.91	320.69	347.52	373.45	386.06	396.99
240	281.45	295.18	319.90	346.57	372.31	384.84	395.68
270	280.83	294.54	319.21	345.74	371.31	383.78	394.54
300	280.27	293.96	318.59	344.99	370.42	382.83	393.52
360	279.32	292.98	317.53	343.72	368.89	381.20	391.77
Third step							
10	448.87	470.05	497.71	530.03	558.36	573.07	590.98
30	435.04	455.22	481.72	512.93	540.16	554.76	572.90
60	426.74	446.33	472.14	502.70	529.27	543.79	562.05
90	422.03	441.29	466.71	496.90	523.11	537.57	555.89
120	418.76	437.79	462.94	492.87	518.82	533.25	551.61
150	416.25	435.10	460.05	489.79	515.54	529.94	548.33
180	414.22	432.94	457.72	487.30	512.89	527.27	545.67
210	412.52	431.12	455.77	485.21	510.67	525.03	543.45
240	411.06	429.56	454.09	483.42	508.77	523.11	541.54
270	409.78	428.19	452.62	481.85	507.10	521.42	539.87
300	408.65	426.98	451.31	480.45	505.62	519.93	538.38
360	406.69	424.89	449.07	478.05	503.06	517.35	535.82

Characterization of BHT

The XRD pattern of BHT prepared by solid state reactions is presented in Fig. 4. Whilst TNTs display very broad diffraction peaks, the BHT sample exhibited very sharp diffraction peaks indicating a well-crystallized structure. All the reflections of the sample are in agreement with monoclinic hydrogen trititanate ($H_2Ti_3O_7$, PDF No: 00-041-0192).

The TG/DTG curves of BHT showed mass losses in three dehydration stages in the range of 100–640 °C at 15 °C min^{-1} heating rate, similar to the thermogravimetric data of Morgado et al. [29] (Fig. 5). Compared to the TNTs, BHT showed a significantly different thermal

behaviour. The first mass loss of BHT started at 100 °C with a mass loss of 2.97 %, the second mass loss up to 460 °C occured with a mass loss of 2.10 % and the final dehydration with a mass loss of 0.97 % corresponded to dehydroxylation of the BHT. It was observed that these dehydroxylation steps were well pronounced. However, analysis of the DTG curve for TNTs reveals that its dehydroxylation steps were not well pronounced, a difference which can be attributed to the nanocrystalline nature of TNTs [29].

Studies of thermal dehydration kinetics

The activation energy as a function of conversion to each dehydration stage of TNTs is shown in Fig. 6. In the range of 5–90 % of conversion, the activation energies for the first and second dehydration stages are 81.44 ± 15.85 and 82.69 ± 7.46 kJ mol^{-1}, respectively. The activation energy as a function of conversion to each dehydration stage of BHT is shown in Fig. 7. In the range of 10–95 % of conversion, the activation energies for the first, second and third dehydration stages are 115.93 ± 5.40, 137.58 ± 6.47 and 138.97 ± 8.47 kJ mol^{-1}, respectively. The values of activation energies for the all dehydration processes of TNTs were lower than those found for BHT. This means that the TNTs' dehydration reactions need to overcome a lower energy barrier than those of BHT.

The obtained activation energy curves for each stage were used to predict the temperature required to remove water from TNTs and BHT as a function of the conversion and time by means of a model-free algorithm [26]. Tables 1 and 2 show the predicted dehydration temperature values for TNTs and BHT as a function of time for different conversions. It was observed that to remove 99 % of the water from TNTs within 120 min, 100.99 and 473.43 °C are necessary for the first and second steps, respectively. It was observed that to remove 99 % of the water from BHT in the same time 273.46, 402.56 and 551.61 °C are necessary for the first, second and third steps, respectively.

Conclusions

The TNTs were synthesized via the hydrothermal synthesis of titania nanopowder. These experiments were carried out by varying several reaction parameters such as the reaction temperature, the reaction time, NaOH concentration and the acidity of the washing solution. The experimental results suggested that the formation of TNTs was affected strongly by the variation in all of these parameters.

The thermal analysis of TNTs synthesized under optimum conditions was employed to investigate their thermal behaviour and dehydration kinetics. Also, thermal analysis of BHT was carried out in order to clarify the thermal behaviour of TNTs. Whilst the dehydroxylation steps of BHT are well pronounced, those of TNTs are not, possibly due to their nanocrystalline nature. The values of activation energies for the all dehydration processes of TNTs were lower than those found for BHT.

The Vyazovkin model-free method applied in the research provided a sound way of estimating the apparent activation energy for dehydration processes and to predict conversion and isoconversion parameters.

The experimental findings of this study allow for better understanding of the parameters concerning the synthesis of TNTs. The determination of these optimized parameters is significant since they would be practiced in the production of TNTs with varying surface morphologies for all kinds of applications.

Acknowledgements The authors gratefully acknowledge the financial support provided by the Scientific and Technological Research Council of Turkey.

References

1. Kim G-S, Kim Y-S, Seo H-K, Shin H-S. Hydrothermal synthesis of titanate nanotubes followed by electrodeposition process. Korean J Chem Eng. 2006;23:1037–45.
2. Mastan AAK, Ahmedullah SS, Mohamed NM. The effect of hydrothermal growth parameters on titanium dioxide nanomaterial. J Appl Sci. 2011;11:1267–72.
3. Thorne A, Kruth A, Tunstall D, Irvine JTS, Zhou W. Formation, structure, and stability of titanate nanotubes and their proton conductivity. J Phys Chem B. 2005;109:5439–44.
4. Kasuga T, Hiramatsu M, Hoson A, Sekino T, Niihara K. Titania nanotubes prepared by chemical processing. Adv Mater. 1999;11:1307–11.
5. Yang J, Jin Z, Wang X, Li W, Zhang J, Zhang S, Guo X, Zhang Z. Study on composition, structure and formation process of nanotube $Na_2Ti_2O_4(OH)$. Dalton Trans. 2003;3898–901.
6. Ma R, Banda Y, Sasaki T. Nanotubes of lepidocrocite titanates. Chem Phys Lett. 2003;380:577–82.
7. Nakahira A, Kato W, Tamai M, Isshiki T, Nishio K. Synthesis of nanotube from a layered $H_2Ti_4O_9(H_2O)$ in a hydrothermal treatment using various titania sources. J Mater Sci. 2004;39:4239–45.
8. Ou H-H, Lo S-L. Review of titania nanotubes synthesized via the hydrothermal treatment: Fabrication, modification, and application. Sep Purif Technol. 2007;58:179–91.
9. Hoyer P. Formation of titanium dioxide nanotubes array. Langmuir. 1996;12:1411–3.
10. Lee JH, Leu IC, Hsu MC, Chung YW, Hon MH. Fabrication of aligned TiO_2 one-dimensional nanostructured arrays using one-step templating solution approach. J Phys Chem B. 2005;109:13056–9.
11. Kasuga T, Hiramatsu M, Hoson A, Sekino T, Niihara K. Formation of titanium dioxide nanotube. Langmuir. 1998;14:3160–3.
12. Zwilling V, Aucouturier M, Darque-Ceretti E. Structure and physicochemistry of anodic oxide films on titanium and TA6V alloy. Surf Interface Anal. 1999;27:629–37.

13. Tsuchiya H, Macak JM, Taveira L, Balanur E, Ghicov A, Sirotna K, Schmuki P. Self-organized TiO_2 nanotubes prepared in ammonium fluoride containing acetic acid electrolytes. Electrochem Commun. 2005;7:576–80.
14. Tsai CC, Nian JN, Teng H. Mesoporous nanotube aggregates obtained from hydrothermally treating TiO_2 with NaOH. Appl Surf Sci. 2006;253:4193–8.
15. Lee C-K, Liu S-S, Chen H-C. Application of hydrothermal method derived titanate nanotubes as adsorbents. Recent Pat Nanotechnol. 2009;3:203–12.
16. Kasuga T. Formation of titanium dioxide nanotubes using chemical treatments and their characteristic properties. Thin Solid Film. 2006;496:141–5.
17. Niu L, Shao M, Wang S, Lu L, Gao H, Wang J. Titanate nanotubes: preparation, characterization, and application in the detection of dopamine. J Mater Sci. 2008;43:1510–4.
18. Souza MJB, Silva AOS, Aquino JMFB, Fernandes V J Jr, Araújo AS. Kinetic study of template removal of MCM-41 nanostructured material. J Therm Anal Calorim. 2004;75:693–8.
19. Naik YP, Ramarao GA, Banthiya A, Chaudhary D, Arora C. Synthesis and characterization of nano-structured Th12xCexO2 mixed oxide. J Therm Anal Calorim. 2012;107:105–10.
20. Jones DEG, Brousseau P, Fouchard RC, Turcotte AM, Kwok QSM. Thermal characterization of passivated nanometer size aluminium powders. J Therm Anal Calorim. 2000;61:805–18.
21. Robinson PP, Arun V, Manju S, Aniz CU, Yusuff KKM. Oxidation kinetics of nickel nano crystallites obtained by controlled thermolysis of diaquabis (ethylenediamine) nickel(II) nitrate. J Therm Anal Calorim. 2010;100:733–40.
22. Lorençon E, Lacerda RG, Ladeira LO, Resende RR, Ferlauto AS, Schuchardt U, Lago RM. Thermal behavior of carbon nanotubes decorated with gold nanoparticles. J Therm Anal Calorim. 2011; 105:953–9.
23. Xie Y, Liu C, He H, Lu X. Thermal analysis of hydrogen titanate nanotubes prepared by potassium dititanate with water vapour treatment. J Therm Anal Calorim. 2011;. doi:10.1007/s10973-011-1912-z.
24. Kasap S, Tel H, Piskin S. Preparation of TiO_2 nanoparticles by sonochemical method, isotherm, thermodynamic and kinetic studies on the sorption of strontium. J Radioanal Nucl Chem. 2011;289:489–95.
25. Izawa H, Kikkawa S, Kotzumi M. Ion exchange and dehydration of layered titanates, $Na_2Ti_3O_7$ and $K_2Ti_4O_9$. J Phys Chem. 1982; 86:5023.
26. Vyazovkin S, Wright CA. Model-free and model-fitting approaches to kinetic analysis of isothermal and nonisothermal data. Thermochim Acta. 1999;340:53.
27. Vyazovkin S, Goriyachko V. Potentialities of software for kinetic processing of thermoanalytical data by the isoconversion method. Thermochim Acta. 1992;194:221.
28. Vyazovkin S, Lesnikovick AI. Conversion of kinetic data from the temperature-dependent degree of conversion to the time dependent degree of conversion. Russ J Phys Chem. 1988; 62:2949–53.
29. Morgado E Jr, Jardim PM, Marinkovic BA, Rizzo FC, Abreu MAS, Zotin JL, Araujo AS. Multistep structural transition of hydrogen trititanate nanotubes into TiO_2-B nanotubes: a comparison study between nanostructured and bulk materials. Nanotechnology. 2007;18:495710.